# Measurements of Electron Thermal Diffusivity in Laser-Ablated Impurity Injection Experiments

J O'Rourke, R Giannella.

JET Joint Undertaking, Abingdon, Oxon, OX14 3EA.

# Measurements of Electron Thermal Diffusivity in Laser-Ablated Impurity Injection Experiments

J O'Rourke, R Giannella.
JET Joint Undertaking, Abingdon, Oxfordshire, OX14 3EA, UK.

## 1. SUMMARY

The radiation induced by the laser ablation ("blow-off") of non-recycling impurities gives rise to a transient perturbation of the electron temperature. The inward propagation of this "cold pulse" can be used to determine a thermal diffusivity, $\chi_e^{cp}$. The impurity ablation technique presents a number of advantages with respect to other perturbation techniques for the analysis of transport in tokamaks. In particular, the radial zone in which $\chi_e^{cp}$ is measured does not vary strongly with plasma parameters and effects arising from perturbations of quantities other than the electron temperature are minimal.

A salient feature of the data is that the amplitude of the perturbation does not decay as the cold pulse travels inward. This cannot be attributed to a lack of localisation of the perturbed heat sources. We show that it can be interpreted as the signature of a non-linearity of the electron heat transport equation.

For $0.4 < r/a < 0.8$, $\chi_e^{cp} = 2.5 \pm 1 m^2 s^{-1}$ in 3 MA ohmic discharges, rising to $\chi_e^{cp} = 13\ (+10, -5)\ m^2 s^{-1}$ with 10 MW of ICRF heating.

## 2. INTRODUCTION

- The analysis of "cold pulses" generated by impurity ablation on TFTR was reported in [1].
- The propagation of "cold pulses" following $D_2$ pellet injection has been used previously in JET to determine simultaneously electron and ion thermal diffusivities and the electron particle diffusion coefficient [2].

The laser blow-off technique has a number of attractive features:

- The perturbed source is well localized at the plasma periphery because:
  - the radiation comes mostly from the lower ionization stages,
  - the rate of impurity particle transport is much slower than that of heat transport ($D_I \ll \chi_e^{cp}$).

- The measurement region does not vary strongly with plasma parameters, so that dependences on plasma parameters and any explicit radial dependence are more easily separated. By contrast:
  - the analysis of heat pulse propagation is performed in a region just beyond the mixing radius which varies as $q_a$ is varied.
  - the analysis of pellet-induced cold pulses is performed inside of the pellet penetration radius which varies strongly with electron temperature.
- It is empirical observation that the amplitude of the perturbation does not decay with distance. This implies that the measurement region is not limited by signal-to-noise considerations.
- The electron density perturbation is very small. This minimizes any effects arising from coupling of the heat and particle transport.
- Since the perturbation does not arise from a plasma instability (like a sawtooth), there is no question of the transport being affected by changes in the magnetic topology.
- The timing and amplitude of the perturbation are experimentally controllable.
- Heat and (impurity) particle transport can be studied simultaneously. Tritium doping of the high-Z impurities would allow the simultaneous measurements of $D_T$ , $D_I$ and $\chi_e^{cp}$.

A limitation of the technique is given by the finite rise time of the edge temperature perturbation $\tau_{pert}$. Values of $\chi_e^{cp}$ that give propagation times $\tau_{trans}$ short with respect to $\tau_{pert}$ cannot be resolved. For JET, this means that values of $\chi_e^{cp} > 8m^2/sec$ cannot be measured accurately.

## 3. EXPERIMENT

- Perturbations are generated by the injection of Ni atoms by laser ablation [3]. Typically ~ $5.X10^{17}$ impurity atoms penetrate the plasma following laser blow-off.
- The evolution of the electron temperature is followed using a 12-channel grating polychromator. The spatial resolution of this instrument is 5 cm and the noise in the data is 10-20 eV.
- Impurity injection causes a sharp drop of $T_e$ at the plasma edge (~ 100 eV) followed by a more gradual reheat. See figure 1.
- The perturbation propagates inward. The time-to-minimum clearly increases as the minor radius decreases.
- A key feature of the data is that the amplitude of the perturbation *increases* with distance from the plasma edge.
- Parameters were scanned in the ranges $2 < I_p < 4$ MA, and $0 < P_{AUX} < 10$ MW.

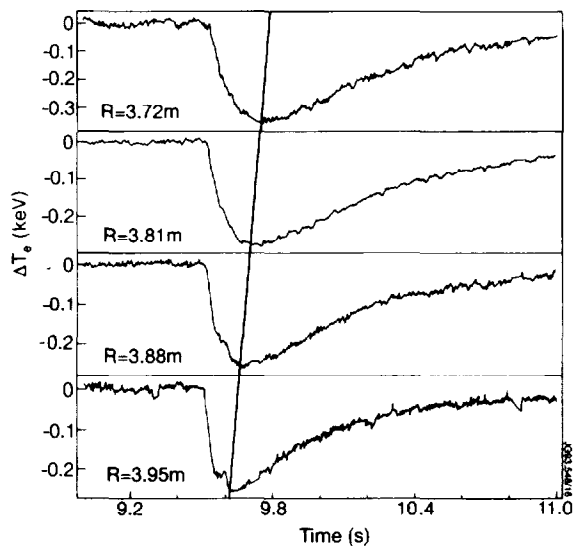


*Figure 1: Temperature perturbation induced by Ni injection in pulse 27401.*

## 4. ANALYSIS

- The heat equation is solved numerically (without linearization) for assumed values and functional forms of $\chi_e^{cp}$. The input power is used as a free parameter to satisfy the initial steady-state conditions. Thus $\chi_e^{cp}$ represents the *incremental* heat diffusivity.
- An outer channel of the polychromator (at R = 3.8-3.9 m) is taken as forced boundary condition: the power radiated outside this radius is used as feedback to reproduce the observed temperature evolution on this channel.
- The assumption that the perturbed heat sources/sinks are outside the reference channel is crucial to the analysis. It is justified because:
  - The radiation comes from relatively low ionization stages that only exist near the plasma boundary.
  - Bolometric measurements confirm the edge-localized nature of the perturbation. See figure 2.
  - The heat transport is *a posteriori* verified to be more rapid than the impurity particle transport [3]. Therefore the heat source effects and the heat transport effects are separated temporarily as well as spatially.
  - Numerical checks show that if the perturbed heat source is not strictly within the reference radius, the results are not altered significantly.
- The experiments with auxiliary heating were not in steady-state at the time of the impurity injection. This necessitates a careful subtraction of the background temperature evolution and introduces additional uncertainties in the analysis of these discharges. See figure 3.

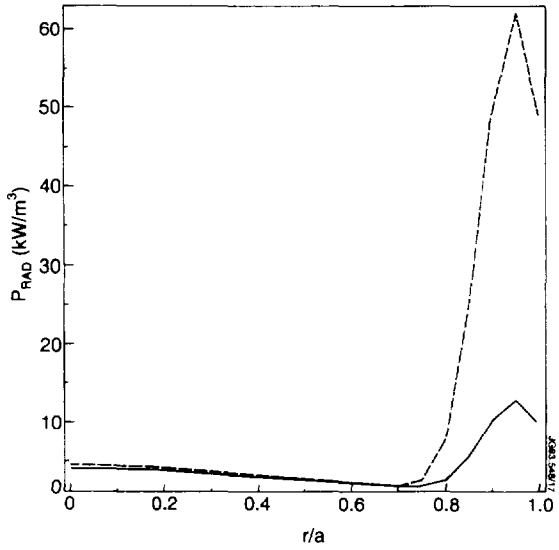


*Figure 2: Radiated power profile (obtained by Abel inversion of bolometric data), before (solid line) and following (dashed line) impurity injection.*

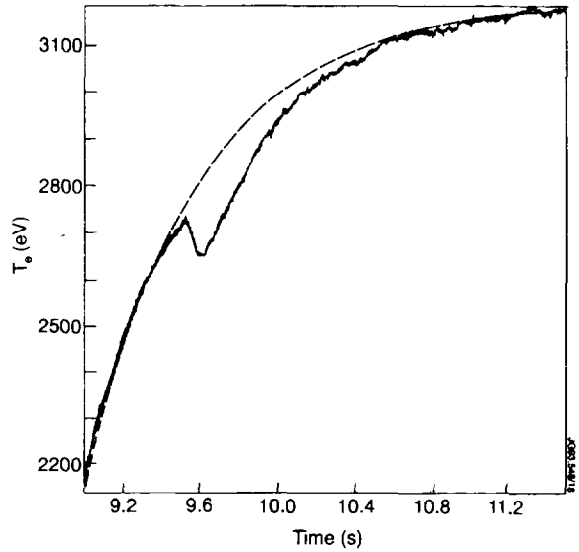


*Figure 3: Evolution of the electron temperature in pulse 27417 following the application of 6 MW of ICRF power. Also shown is the exponential baseline used to determine the perturbation produced by Ni injection at 9.5 sec..*

- $\chi_e^{cp}$ is varied to minimize $<(\tilde{T}_e^{sim} - \tilde{T}_e^{exp})^2>$ at smaller minor radii. The error on the best fits obtained in this manner is of the order of the noise of the data (10-20 eV).
- An additional consistency check is provided by the radiated power feedback which is compared with the measured evolution of $P_{rad}$. See figure 4.
- Sawteeth limit the usefulness of the innermost channels of the polychromator. Thus the measurement of $\chi_e^{cp}$ is effectively carried out in a radial zone between the mixing radius and the radius where the perturbation of the heat source becomes dominant. In practice this corresponds to $0.4 < r/a < 0.8$. See figure 5.

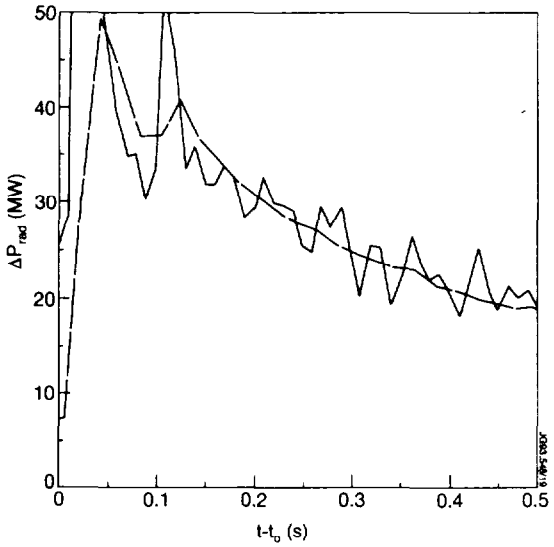


*Figure 4: Change in the total radiated power as a function of time in pulse 27401 (a) dashed line– data and (b) solid line– simulation.*

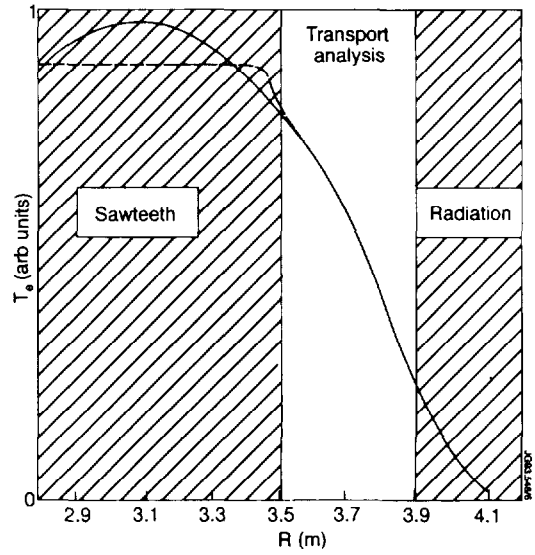


*Figure 5: Schematic illustration of the radial zone in which the transport analysis is carried out.*

## 5. RESULTS

- The temperature perturbation at each radius is characterized by two parameters: the time at which the minimum is reached and the amplitude of the perturbation.
- The "time-to-trough" can be fitted by adjusting the value of $\chi_e$ in the simulations.
- A salient feature of these data is that the amplitude grows as it propagates inward.
  - As discussed in the previous section this cannot be attributed to a perturbation of the heat source in the measurement region.
  - It does not result from any geometrical effect related to the fact that the perturbation is propagating into a decreasing volume.
  - It is too large to be caused by coupling of the electron heat and particle transport [4].
  - It *does* arise naturally in some non-linear transport models.
- We first consider a local transport model, in which the heat diffusivity scales with the inverse temperature scale length, $L_T^{-1} = -\nabla T_e / T_e$:

$$\chi_e^{cp} = \chi_0 \left( \frac{L_{T0}}{L_T} \right)^{\alpha}$$

Figure 6 shows the data and simulation at several radii, for an ohmically heated 3MA discharge. Here $\chi_0 = 1\ m^2\ sec^{-1}$ and $\alpha = 2$. Also shown is the simulation with $\chi_0 = 3\ m^2\ sec^{-1}$ and $\alpha = 0$. The introduction of a dependence on the temperature scale length has the effect of:

- increasing the linearized diffusivity, $\chi_e^{lin} = (1 + \alpha)\chi_0$ and
- increasing the pulse amplitude as the perturbation diffuses inward.

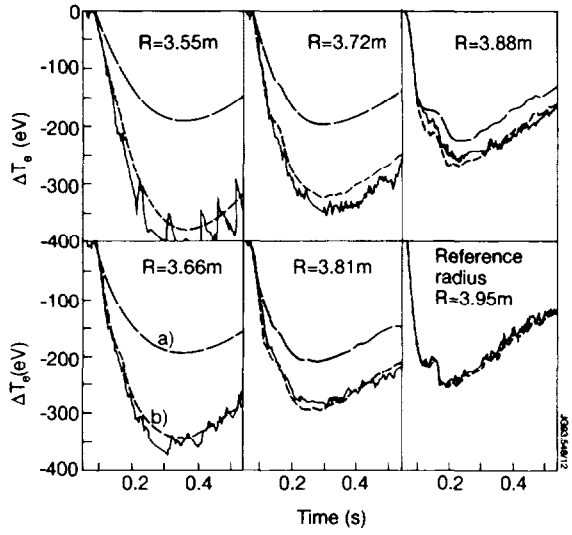


*Figure 6: Temperature perturbation in pulse 27401. Also shown are simulations asuming (a) no dependence on $L_T$ ($\alpha = 0$, $\chi_0 = 3m^2\ sec^{-1}$) and (b) a quadratic dependence on $L_T$ ($\alpha = 2$, $\chi_0 = 1m^2\ sec^{-1}$).*

- Figures 7 and 8 show the variation of $\chi_e^{lin}$ and $\alpha$ with volume averaged electron temperature in a series of 3MA discharges with which the ICRF power was scanned in the range 0-10 MW. Both $\chi_0$ and $\chi_e^{lin}$ increase with increasing temperature. However, the ratio $\chi_e^{lin}/\chi_0$ approaches unity at high temperatures ($\alpha$ becomes small). This result is analogous to the observation that the enhancement of the sawtooth heat pulse diffusivity over the power balance diffusivity is greatest in ohmic discharges [5]. Measurements of $D_I$ in the outer portion of these discharges shows a similar degradation (from 1 to 3 $m^2$/sec) with electron temperature [6].

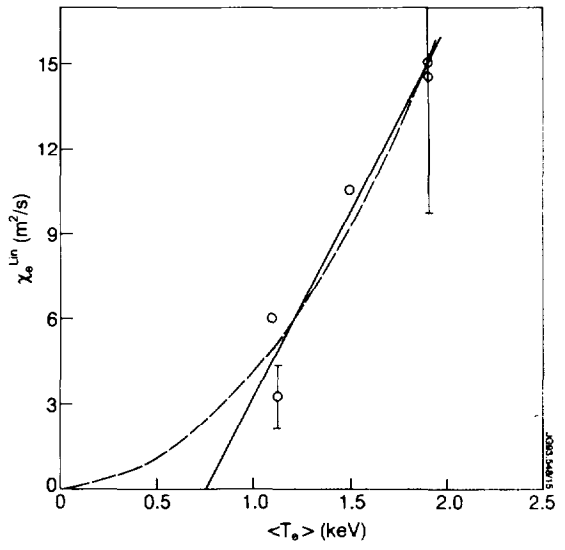


*Figure 7: $\chi_e^{lin}$ versus volume-averaged electron temperature in a power scan of 3MA discharges.*

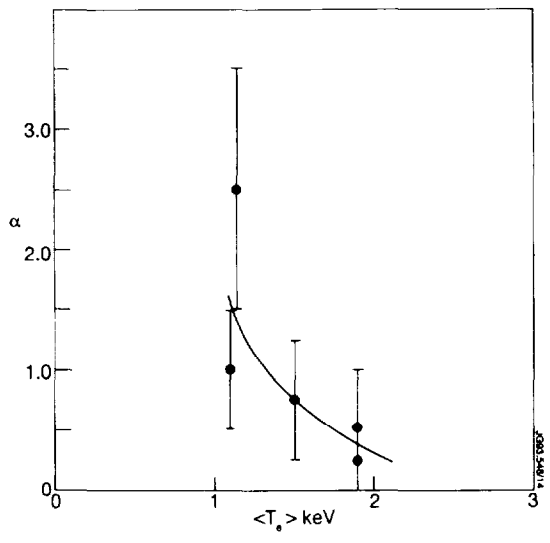


*Figure 8: α versus volume-averaged electron temperature in a power scan of 3MA discharges.*

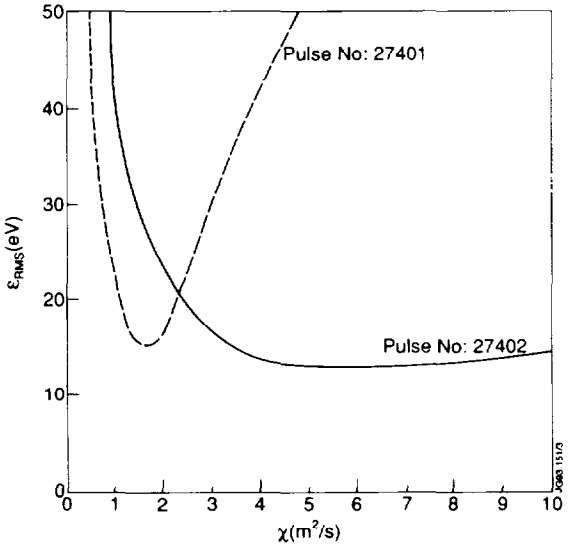


*Figure 9: RMS error versus $\chi_0$ for an ohmic discharge (27401) and a discharge with 9 MW of ICRF heating.*

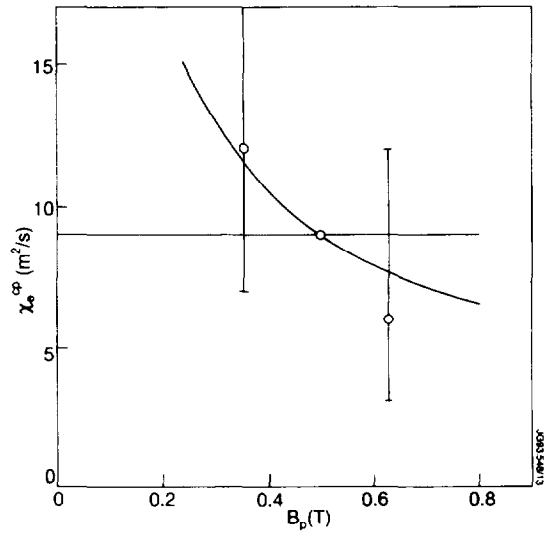


*Figure 10: $\chi^{cp}$ versus poloidal field (obtained in a 2-4 MA current scan with approximately 6 MW of ICRF power). Also shown are the expected variations if $\chi_e^{cp} \sim T_e^2 / B_p^2$ (solid line) and $\chi_e^{cp} \sim B_p^0$, (dashed line).*

- $\chi_0$ and α are varied independently to obtain the best fit of the simulations to the data. The limitations of the impurity injection technique are exemplified by considering $\varepsilon_{rms}$, the RMS deviation between simulations and data as a function of $\chi_0$. See figure 9. Here α is taken to be 1, and the pulse amplitudes are normalized to minimize $\varepsilon_{rms}$ (this is equivalent to fitting the time-to -trough). For an ohmic pulse (#27401), the optimal value of $\chi_0$ is low and the minimum in $\varepsilon_{rms}$ is well defined. Pulse

#27402 has a considerably higher $\chi_0$ , and this cannot be resolved very accurately because the characteristic time of the temperature perturbation at the edge is not short compared with the pulse propagation time. Thus the error in the detemination of $\chi_0$ increases rapidly with $\chi_0$ and becomes asymmetric. Ultimately, only a lower bound on $\chi_0$ can be given.

- Figure 10 plots $\chi_e^{cp}$ versus poloidal field in the measurement zone. Although the data indicate a trend toward improved confinement at higher currents, the large error bars and the strong dependence on electron temperature discussed above mean that no firm conclusion can be drawn.

## 6. DISCUSSION

- What features of the above model lead to an increase of the pulse amplitude as it propagates inward? Consider a heat diffusivity of the form:

$$\chi_e = CT_e^{\alpha}(\nabla T_e)^{\beta}$$

For a radially constant heat source and C the steady-state temperature profile has the property that

$$\frac{\Delta T_{e0}}{T_{e0}} = \frac{\Delta T_{ea}}{T_{ea}} \bullet \left[\frac{T_{ea}}{T_{e0}}\right]^{\frac{\alpha+\beta+1}{\beta+1}}$$

where $\Delta T_{ea}$ is an imposed change in the boundary condition and $\Delta T_{eo}$ is the resulting change in the central temperature. If $\alpha = 0$, $\Delta T_{eo} = \Delta T_{ea}$. However, if $\alpha < 0$, the change in the central temperature is larger than the change in the edge temperature. If $\alpha = -(\beta + 1)$, then $\frac{\Delta T_{e0}}{T_{e0}} = \frac{\Delta T_{ea}}{T_{ea}}$, so that the *relative* change in the central temperature is equal to the *relative* change in the edge temperature.

Thus C determines the steady-state or power balance diffusivity, $\beta$ determines the enhancement of $\chi_{perturbation}$ over $\chi_{power\text{-}balance}$, $\alpha + \beta$ defines the degree of confinement degradation with power, and $\alpha/(\beta + 1)$ determines the degree of "profile consistency".

- Another model that is capable of reproducing the increasing amplitude of a propagating cold pulse is the non-local model proposed by Parail et al. and discussed at this meeting in the context of the L-H transition and heat pulse propagation. It assumes that the heat diffusivity across the entire radius is governed by electron temperature near the plasma edge. Taking

$$\chi_e^{cp} = \chi_0 \left(\frac{T_{a0}}{T_a}\right)^{\alpha}$$

with $\alpha \sim 0.5$ leads to simulations that are indistinguishable from those shown in figure 6. The very

rapid pulse propagation observed at high auxiliary power levels also arises naturally in this non-local model. However it is difficult to see how such a form for $\chi_e$ can reproduce the enhancement of the sawtooth heat pulse diffusivity over the power balance value. Therefore, it would appear that some dependence of $\chi_e$ on the temperature gradient should be retained in a transport model if it is to reproduce the entire range of experimental observations.

## 7. CONCLUSIONS

- Impurity blow-off can be used for the anlysis of thermal transport as well as impurity transport.
- $\chi_e^{cp} > \chi_{eff}$, $\chi_e^{cp} \sim 3D_I$
- Strong power degradation is observed, compatible with a threshold.
- Current dependence masked by large error bars and power degradation.
- Radial dependence of pulse amplitude suggests $\chi_e^{cp} \sim (-\nabla T_e/T_e)^{\alpha}$. This non-linearity is of 'profile consistent' character: linear diffusion equations do not give rise to pulses which grow in amplitude as they get further from the initial perturbation.

## 8. REFERENCES


[1] M W Kissick et al,. Bull. Am. Phys. Soc. 37 (1992) 1483.

[2] A D Cheetham et al., 12th IAEA, Nice, 1988, Nuclear Fusion Supplement 1 (1989) 483.

[3] D Pasini et al., 19th EPS Conf. on Contr. Fus. and Plasma Phys., Innsbruck, 1992, Vol.16C, pt.1, p.283.

[4] J C M de Haas et al., Nuclear Fusion 31 (1991) 1261.

[5] B J D Tubbing et al., Nuclear Fusion 26 (1986) 849.

[6] R Giannella et al, 20th EPS Conf on Contr Fus and Plasma Phys, Lisbon, 1993, vol.17c, pt.1, p.43.